Proceedings of the

SECOND INTERNATIONAL SYMPOSIUM ON

NEUTRON CAPTURE GAMMA RAY SPECTROSCOPY

AND RELATED TOPICS

September 2–6 1974, Petten, the Netherlands

Neutron Capture Gamma-Ray Spectroscopy

Published by Reactor Centrum Nederland, Petten, the Netherlands

March 1975

SHELL-MODEL APPROACH TO THE THEORY OF LOW-ENERGY NEUTRON CAPTURE

J. Cugnon and C. Mahaux†, University of Liège, Belgium

ABSTRACT

We first review some applications of the shell-model approach to the giant resonances and then turn to the region of isolated resonances, with main emphasis on deviations from the statistical model due to channel capture. We write down various parametrizations for the scattering matrix, and discuss the identification of the corresponding resonance and background parameters with theoretical quantities. The relationship between the present formulation and the work of Lane, Lynn and Mughabghab is exhibited, both formally and numerically.

1. Introduction

During the last decade, much effort has been devoted to the qualitative and quantitative description of resonance reactions by means of models which had previously been developed for bound nuclear states. This progress has been triggered by Feshbach's theory [1,2]), which contains the shell-model approach [3]) as a particular case. In the present context, the expression "shell-model approach" (SMA) covers all formulations in which a Hamiltonian is diagonalized in a space of functions, which include scattering states, and are generated from a single-particle potential well of finite depth. Most of the recent "dynamical theories" only differ by the techniques used for solving this problem. The main features of the SMA are recalled in sect. 2, which also establishes our notation. Comprehensive reviews [3,4]) exist of the shell-model calculations performed prior to 1972 in the region of the giant resonances. Accordingly, this topic is only briefly discussed in sect. 3, with emphasis on recent progress. The SMA to radiative capture in the region of isolated resonances is described in sect. 4. There, we also introduce the channel capture model, which bears much resemblance with the valence capture model of Lane and Lynn [5]). In sect. 5, we discuss the identification of the theoretical quantities with the resonance parameters obtained from the analysis of the data. Some numerical results are given in sect. 6.

† presented by C. Mahaux

2. Shell-model approach

2 a. The model

We write the full Hamiltonian as the sum of a residual interaction V and of an independent particle Hamiltonian H_o. We call ϕ_j and χ_E^c, respectively, the normalized bound and scattering eigenstates of H_o

$$H_o\,\phi_j = E_j\,\phi_j\ ,\quad H_o\,\chi_E^c = E\,\chi_E^c\ ,\quad \langle\chi_E^c|\chi_{E'}^{c'}\rangle = \delta_{cc'}\,\delta(E-E')\ . \tag{1}$$

The upper index c refers to the channel quantum numbers. For simplicity, we take s-wave neutron channels and 0^+ target and residual states θ_c. Moreover, we omit explicit reference to antisymmetrization and write

$$\chi_E^c = t_c(r;E)\theta_c\ ,\quad t_c(r;E) \to 2^{\frac{1}{2}}\,(\pi\hbar v_c)^{-\frac{1}{2}}\sin(k_c r + \delta_o^c)\ , \tag{2}$$

where δ_o^c is the model potential scattering phase shift due to the single-particle potential v_o; k_c is the wave number and v_c the velocity. We have absorbed a factor r^{-1} into θ_c.

The SMA consists in diagonalizing H in the space of functions spanned by the basis $\{\phi_j, \chi_E^c\}$ [3]. This amounts to finding the coefficients $\underline{a}$ and $\underline{b}$ of the expansion

$$\psi_E^c = \sum_j b_E^c(j)\phi_j + \sum_{c'}\int dE'\ a_E^c(E';c')\chi_{E'}^{c'} \tag{3}$$

which are such that

$$\langle\psi_E^c\,|H_o + V|\,\psi_{E'}^{c'}\rangle = E\,\delta_{cc'}\,\delta(E-E')\ . \tag{4}$$

The upper index $\underline{c}$ refers to the asymptotic behaviour of the radial wave function $u_{c'}^c$:

$$u_{c'}^c(r;E) = (\theta_{c'}|\psi_E^c\rangle\ . \tag{5}$$

Here, the round bracket indicates an integration over the coordinates contained in $\theta_{c'}$:

$$u_{c'}^c(r;E) \to (2/\pi\hbar)^{\frac{1}{2}}\{v_c^{-\frac{1}{2}}\sin k_c r\,\delta_{cc'} + K_{cc'}\,v_{c'}^{-\frac{1}{2}}\cos k_{c'}r\}\ . \tag{6}$$

The S-matrix is given by

$$S = (1+iK)(1-iK)^{-1}\ . \tag{7}$$

2 b. Methods of solution

In the coupled-channel method [3,6-8], a set of coupled integro-differential equations for the radial wave functions $u_{c'}^c$ is constructed. The method is in practice limited to about 20 channels; the effect of the omitted channels can be simulated by using a complex potential well v_o. The method is purely numerical in character,

but accurate; it offers a convenient reference for testing various approximation schemes.

Another method consists in deriving a set of coupled integral equations for the coefficient $\underline{a}$ and $\underline{b}$ in eq. (3). These equations involve the matrix elements

$$V_{jm} = \langle\phi_j|V|\phi_m\rangle\ ,\quad V_j^c(E) = \langle\phi_j|V|\chi_E^c\rangle\ , \tag{8}$$

$$V_{EE'}^{cc'} = \langle\chi_E^c|V|\chi_{E'}^{c'}\rangle\ . \tag{9}$$

The equations can be solved by discretization or by treating the channel-channel coupling in perturbation theory [3,7]. A useful approximation scheme is the factorization method. It is based on the fact that in the internal region of the nucleus, the energy dependence of $t_c(r;E)$ (eq. (2)) can be factorized

$$t_c(r;E') \approx f_c(E';E)\,t_c(r;E)\ ;\quad f_c(E,E) = 1\ . \tag{10}$$

Because of the short-range nature of the residual interaction, the approximation (10) can be used in the matrix element of V. For instance, one can make the following approximation in the principal value integral

$$\Delta_{jm}^c(E) = \int dE'\ (E-E')^{-1}\,V_j^c(E')\,V_m^c(E') \tag{11}$$

$$\approx F_c(E)\,V_j^c(E)\,V_m^c(E)\ , \tag{12}$$

where

$$F_c(E) = \int dE'\ (E-E')^{-1}\,f_c^2(E';E)\ . \tag{13}$$

This method can be improved and turns out to be convenient and accurate [9-11]. It will be helpful in sects. 4 and 5 below.

3. Giant resonances

The resonances arise from the coupling (V_j^c) of the bound model states ϕ_j to the scattering states χ_E^c. Dynamical calculations are possible only when the nature of at least a fraction of the physical resonance states can be guessed. This is rarely the case above threshold, except mostly for the isobaric analog resonances and the giant dipole resonances. Thus, most numerical applications of the SMA concern these two cases. In particular, radiative capture cross sections in the region of the giant dipole resonances in ^{12}C, ^{16}O, ^{40}Ca, ^{90}Zr and ^{208}Pb have been calculated, in the subspace of one particle-one hole (1p-1h) configurations [4,6-8,10]. The characteristic feature of these calculations is that they yield too few resonance peaks, which are moreover too high. Their heights become satisfactory if a complex potential well v_o is used [6,8]. The imaginary part of

v_o simulates the existence of omitted open channels. The latter point is confirmed by the results of ref. [10]). There, an enlarged basis was used for ^{12}C, obtained by coupling a nucleon to realistic states in ^{11}B and ^{11}C. With twelve open channels, no imaginary part was needed; moreover, Birkholz [10]) achieves an impressive agreement with the experimental fine structure. He used an improved version of the factorization method.

Wang and Shakin [12]) could account for the fine structure of the giant dipole resonance in ^{16}O, by including 3p-3h excited states [13]). They first claimed that the detailed reproduction of the data requires a large E2 amplitude [14]), tentatively ascribed to a giant quadrupole resonance. However, it now appears that the data can also be fitted by modifying the phase difference between the E1 amplitudes [15]). We note that other candidates for the fine structure levels in ^{16}O are 2p-2h and 4p-4h configurations [16]), or deformed excited states [17]).

Recently, the SMA was applied to odd nuclei, like ^{13}C, ref. [18]). Much interest is also presently devoted to the calculation of giant resonances of higher multipolarity.

4. Isolated resonances

In sect. 4 a, we derive many-level formulas from the SMA. The direct capture model, analogous to the valence capture model of Lane and Lynn [5]) is introduced in sect. 4 b. The relationship with the optical-model is discussed in sect. 4 c.

4 a. Many-level formulas

We only give here the reactance-matrix parametrization, in the one-particle channel ($\underline{c}$) case. The S-matrix parametrization and the many-channel case are discussed elsewhere [19-21]). The real symmetric matrix (see eqs. (1), (8), (11))

$$M_{jm} = (E - E_j)\delta_{jm} - V_{jm} - \Delta^c_{jm} \tag{14}$$

is the natural extension of the secular matrix encountered in the bound state case. By diagonalizing M, we obtain eigenvalues E_λ and states ζ_λ. For simplicity, we neglect the channel-channel coupling V^{cc}_{EE} which can, however, easily be included [19-21]). We define the partial width amplitude [3])

$$\gamma_{\lambda c}(E) = (2\pi)^{\frac{1}{2}} \langle \chi^c_E | V | \zeta_\lambda \rangle \ . \tag{15}$$

The S-matrix is given by [3])

$$S_{cc} = \exp(2i\delta_o)\,\frac{1 + i\,Q_{cc}}{1 - i\,Q_{cc}} \ , \tag{16}$$

$$Q_{cc} = \frac{1}{2}\sum_\lambda \frac{\gamma^2_{\lambda c}}{E_\lambda - E} \ . \tag{17}$$

We dropped the upper index $\underline{c}$ on δ^c_o. The standing wave function $\tilde{\Psi}^c_E$ is given by

$$\tilde{\Psi}^c_E = \chi^c_E + (2\pi)^{-\frac{1}{2}} \sum_\lambda \frac{\gamma_{\lambda c}(E)}{E - E_\lambda} Z_\lambda \tag{18}$$

$$\to 2^{\frac{1}{2}} (\pi\hbar v_c)^{-\frac{1}{2}} \{\sin(k_c r + \delta_o) + Q_{cc}\cos(k_c r + \delta_o)\}\,\theta_c \ , \tag{19}$$

where the expression of the (standing) resonance state Z_λ reads

$$Z_\lambda = \zeta_\lambda + (2\pi)^{-\frac{1}{2}} \int dE'\ (E - E')^{-1}\ \gamma_{\lambda c}(E')\chi^c_{E'} \ . \tag{20}$$

For radiative capture into a final state Ψ_f, we have [20])

$$S_{cf} = 2i \exp(i\delta_o)\,\frac{Q_{cf}}{1 - i\,Q_{cc}} \ , \tag{21}$$

$$Q_{cf} = Q^{(o)}_{cf} + \frac{1}{2}\sum_\lambda \frac{\gamma_{\lambda c}\,\rho_{\lambda f}}{E_\lambda - E} \ , \tag{22}$$

$$Q^{(o)}_{cf}(E) = -\langle \Psi_f | D | \chi^c_E \rangle \ , \tag{23}$$

$$\rho_{\lambda f} = \gamma_{\lambda f} + {}^{(1)}\gamma_{\lambda f} \ , \tag{24}$$

$$\gamma_{\lambda f} = -\pi^{-1} \int dE'\ (E - E')^{-1}\ \gamma_{\lambda c}(E')\ Q^{(o)}_{cf}(E') \ , \tag{25}$$

$${}^{(1)}\gamma_{\lambda f} = \left(\frac{2}{\pi}\right)^{\frac{1}{2}} \langle \Psi_f | D | \zeta_\lambda \rangle \ . \tag{26}$$

Here, D is the dipole operator, suitably normalized. We have decomposed the photon width amplitude into two parts; $\gamma_{\lambda f}$ gives the contribution of the channel configuration χ^c_E contained in the resonance state Z_λ. In view of eqs. (23) and (25), it is natural to associate $\gamma_{\lambda f}$ with "channel capture".

4 b. Channel capture model

This model consists in assuming that [19,20]) $\gamma^2_{\lambda f} >> {}^{(1)}\gamma^2_{\lambda f}$. The integral over E' in eq. (25) can be transformed in an integration over radial variables $r_<$ and $r_>$, with standard notations of Green's function theory. The radial variable r in the matrix element $\gamma_{\lambda c}(E')$ is restricted to the internal region (IR), because of the short-range nature of V. We denote by R_o the nuclear radius and define the IR by $r < R_o$. Thus, the external region (ER)

i.e. the values $r_> > R_o$, enters only in $Q_{cf}^{(o)}$. The contribution of the ER can thus be approximated by

$$\{\gamma_{\lambda f}\}_{ER} \simeq - \gamma_{\lambda c} \langle \Psi_f | D | v_c(r;E)\theta_c \rangle_{ER} \quad , \tag{27}$$

where $v_c(r;E)$ is the single-particle scattering state which has the asymptotic behaviour

$$v_c(r;E) \to 2^{\frac{1}{2}} (\pi\hbar v_c)^{-\frac{1}{2}} \cos (k_c r + \delta_o) \tag{28}$$

The contribution of the IR ($r_<$ and $r_>$ smaller than R_o) can be obtained from the factorization approximation (10) - (13)

$$\{\gamma_{\lambda f}\}_{IR} \simeq \pi^{-1} F_c \gamma_{\lambda c} \langle \Psi_f | D | \chi_E^c \rangle_{IR} \quad . \tag{29}$$

We introduce the wave function

$$W_E^c = \{\frac{F}{\pi} \{t_c(r;E)\}_{IR} - \{v_c(r;E)\}_{ER}\} \theta_c \quad , \tag{30}$$

and write

$$\gamma_{\lambda f} / \gamma_{\lambda c} \simeq \langle \Psi_f | D | W_E^c \rangle \quad . \tag{31}$$

We see that the channel capture model leads to a correlation between photon and particle widths. This is in keeping with the findings of Lane and Lynn [5]), who used a very similar model. In their work, however, the ratio of the photon and particle widths is expressed in terms of optical-model wave functions, while eq. (31) involves a real potential well. Lane and Mughabghab [22]) have recently given a framework-independent derivation of the Lane-Lynn result. In sect. 4 c, we show how this alternative form can be derived from eq. (31).

4 c. Relation with optical-model

Lane and Mughabghab assume that [22])

$$u_{c,opt}(r;E) = u_c^c(r;E + iI) \quad , \tag{32}$$

where $u_c^c(r;E)$ is defined in eq. (5), while $u_{c,opt}$ is the optical-model wave function normalized as follows

$$u_{c,opt}(r;E) \to 2^{\frac{1}{2}} (\pi\hbar v_c)^{-\frac{1}{2}} \{\sin k_c r + \tan \delta_{opt} \cos k_c r\} \quad . \tag{33}$$

In the ER, eq. (32) derives from the definition of the optical-model potential (OMP). In the IR, it implies a specific choice among the variety of OMP. We denote by $\tilde{u}_c^c(r;E)$ the radial part of $\tilde{\psi}_E^c$ (Eq. (18)). We have

$$\{\tilde{u}_c^c(r;E + iI)\}_{ER} \to \sin (k_c r + \delta_o) + \tan (\delta_{opt} - \delta_o) \cos (k_c r + \delta_o) \tag{34}$$

In the IR, and with the help of the factorization assumption (10), eqs. (18) and (20) yield

$$\{\tilde{u}_c^c(r;E)\}_{IR} \simeq \{1 - \frac{F}{\pi} Q_{cc}(E)\} t_c(r;E) \quad . \tag{35}$$

Using $Q_{cc}(E + iI) = \tan (\delta_{opt} - \delta_o)$, and an assumption similar to eq. (32), namely

$$\tilde{u}_c^c(r;E + iI) = \frac{\cos \delta_{opt}}{\cos (\delta_{opt} - \delta_o)} u_{c,opt}(r;E) \quad , \tag{36}$$

we find [21]) that eq. (31) can be written in the form

$$\frac{\gamma_{\lambda f}}{\gamma_{\lambda c}} = \frac{\mathrm{Im} \{\langle \Psi_f | D | u_{c,opt}\, \theta_c \rangle \cos \delta_{opt} / \cos (\delta_{opt} - \delta_o)\}}{\mathrm{Im} \tan (\delta_{opt} - \delta_o)} \quad . \tag{37}$$

This result reduces to the Lane-Mughabghab relation [22]) in the limit $\delta_o \to 0$. We return to this point in sect. 5 a below.

5. Interpretation of phenomenological resonance parameters

Eqs. (16), (17), (21) and (22) give a parametrization of the cross section which is model dependent, via the appearance of a model potential scattering phase shift δ_o. Hence, it is useful to establish the relationship between these "theoretical" resonance parameters and those usually listed in the literature. This was particularly emphasized by Feshbach [23]), and is briefly discussed in sects. 5 a and 6 c. In sect. 5 b, we investigate the connection between the average S-matrix and the correlations between partial widths amplitudes. Sect. 5 c is devoted to the background and direct cross sections.

5 a. Parametrization of the data

The parametrizations in sect. 4 depend upon the choice of v_o. One can write down model-independent parametrizations of S and K (eq. (7)) in terms of their singularities. Lane and Mughabghab [22]) assume that

$$K_{cc'} = K_{cc'}^0 + \frac{1}{2} \sum_\lambda \frac{\omega_{\lambda c}\, \omega_{\lambda c'}}{e_\lambda - E} \quad . \tag{38}$$

This is analogous to eq. (17), where an additional term $Q_{cc}^{(o)} = - \pi V_{EE}^{cc}$ would have appeared if we had not neglected this coupling. In practice, only the one-level forms of eqs. (17), (22), (38) are useful :

$$Q_{cc'} = Q_{cc'}^{(\infty)} + \frac{\gamma_{\lambda c}\, \gamma_{\lambda c'}}{E_\lambda - E} \quad , \tag{39}$$

$$K_{cc'} = K_{cc'}^{(\infty)} + \frac{\omega_{\lambda c}\, \omega_{\lambda c'}}{e_\lambda - E} \tag{40}$$

In this one-level case, the parameters of both parametrizations are easily related. For instance, one has [21])

$$\gamma_{\lambda c} = \omega_{\lambda c} \{\cos \delta_o - \sin \delta_o \, Q_{cc}^{(\infty)}\} \quad , \tag{41}$$

$$\gamma_{\lambda f} = \omega_{\lambda f} - \sin \delta_o \, \omega_{\lambda c} \, Q_{cf}^{(\infty)} \quad . \tag{42}$$

From eqs. (37) and (42) one finds that, in the channel capture model,

$$\frac{\omega_{\lambda f}}{\omega_{\lambda n}} = \frac{\mathrm{Im} \langle \Psi_f | D | u_{c,\mathrm{opt}} \, \theta_c \rangle}{\mathrm{Im} \tan \delta_{\mathrm{opt}}} \quad , \tag{43}$$

which is the Lane-Mughabghab result [22]. From eqs. (31), (41) and (42), one finds

$$\omega_{\lambda f} = \omega_{\lambda c} \{\langle \Psi_f | D | w_E^c \rangle \cos \delta_o - \langle \Psi_f | D | \chi_E^c \rangle \sin \delta_o\} \quad . \tag{44}$$

In the analysis of the data, a potential scattering phase shift δ_o is normally used, which is such that $Q_{cc}^{(\infty)} = 0$. The corresponding "experimental" neutron width can be identified with $\gamma_{\lambda c}^2$ if v_o is chosen such as to fit the experimental background. We return to this point is sect. 6 c. The interpretation of the phenomenological photon width is more delicate [21], since it is usually obtained from an area analysis.

5 b. Correlations and average S-matrix

In eq. (7), we can replace E by $E + iI$. Using the matrix notation $\langle A \rangle = \langle A^R \rangle + i \langle A^I \rangle = A(E + iI)$, we find, from eq. (7),

$$\langle K^I \rangle = \frac{1}{2} \{\frac{1}{2} + \langle S^R \rangle + \langle S^I \rangle \{\frac{1}{2} + \langle S^R \rangle\}^{-1} \langle S^I \rangle\}^{-1} - \frac{1}{2} \quad . \tag{45}$$

If we assume that

$$\langle K_{cc'} \rangle = - \frac{\pi}{d} \overline{\omega_{\lambda c} \, \omega_{\lambda c'}} \quad , \tag{46}$$

with familiar notations, eq. (45) shows that the "correlations" are entirely determined by the average S-matrix [21,22,24]. In the case of radiative capture, eq. (45) yields the Lane-Mughabghab result [22] if assumption (32) is made.

5 c. Background and direct cross sections

We call $S_{nf}^{(\infty)}$ the value of S_{nf} away from E_λ or e_λ . Lane and Mughabghab [22] assume that eq. (32) holds and, furthermore, that $K_{nf}^{(\infty)} = \langle K_{nf}^R \rangle$; they obtain

$$S_{nf}^{(\infty)} = - 2 i \frac{\mathrm{Re} \langle \Psi_f | D | u_{c,\mathrm{opt}} \, \theta_c \rangle}{1 - i \, \mathrm{Re} \tan \delta_{\mathrm{opt}}} \quad . \tag{47}$$

In the SMA, one can make similar, but not entirely equivalent, assumptions, namely eq. (36) and $Q_{nf}^{(\infty)} = \langle Q_{nf}^R \rangle$. From eq. (7), one obtains then [21]

$$S_{nf}^{(\infty)} = - 2 i e^{i\delta_o} \frac{\mathrm{Re} \{\langle \Psi_f | D | u_{c,\mathrm{opt}} \, \theta_c \rangle \cos \delta_{\mathrm{opt}} / \cos (\delta_{\mathrm{opt}} - \delta_o)\}}{1 - i \, \mathrm{Re} \tan (\delta_{\mathrm{opt}} - \delta_o)} \quad . \tag{48}$$

Like in sect. 4 b, one can obtain the other result [21]

$$S_{nf}^{(\infty)} = 2 i e^{i\delta_o} \frac{- \langle \Psi_f | D | \chi_E^c \rangle + Q_{nn}^{(\infty)} \langle \Psi_f | D | w_E^c \rangle}{1 - i \, Q_{nn}^{(\infty)}} \quad . \tag{49}$$

If the potential v_o is chosen in such a way that $Q_{nn}^{(\infty)} = 0$ (see sect. 6 c below), the background value (49) reduces to the direct term

$$S_{nf}^{(o)} = - 2 i \exp (i \delta_o) \langle \Psi_f | D | \chi_E^c \rangle \quad . \tag{50}$$

6. Numerical results

The relations given in sect. 4 are largely equivalent to those contained in refs. [19,20,25], where a parametrization in terms of the complex poles and residues of the S-matrix was used. In the numerical calculations of ref. [20], however, the factorization assumption (10) was carried out up to about $2 R_o$, which is inaccurate at low energy although we saw in sect. 3 that it is quite good in the region of the giant resonances. In sect. 6 a, we compare the quantities (31), (37), (43) and (44) in the case $^{60}Ni(n,\gamma)$. The dependence of these quantities upon mass number is considered in sect. 6 b. The choice of v_o is discussed in sect. 6 c. We compute the background cross section in sect. 6 d. Further results will be published elsewhere [21].

6 a. Photon width in the case $^{60}Ni(n,\gamma)$

In refs. [19,20,25], the potential v_o was taken equal to the real part of the OMP given in ref. [26]. Here, we adopt the same potential and return to this choice in sect. 6 c. The energy dependence of expressions (31), (37), (43) and (44) is shown (in arbitrary units) in fig. 1, for the case $^{60}Ni(n,\gamma)$. We see that the agreement bet-

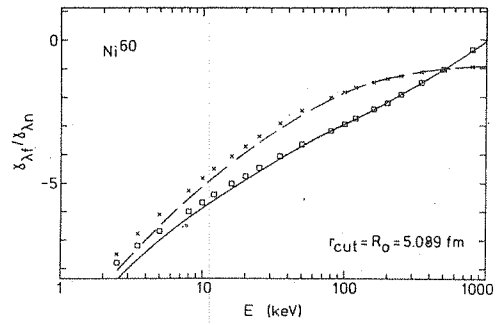

Fig. 1. Comparison between expressions (31) (crosses), (37) (long dashes), (43) (full curve) and (44) (squares).

)

veen (31) and (37), and between (43) and (47), is quite good. The region between R_o and $2\,R_o$ gives the largest contribution to all the matrix elements involved, and the expressions (31) and (44) are fairly insensitive to the precise choice of the cut-off radius r_{cut} delimiting the IR [21]). Similar results are obtained in the case $^{56}Fe(n,\gamma)$ [21]). In the table below, we list the "experimental" resonance parameters (first three columns), and several theoretical photon widths. In the fourth column, we give $\omega^2_{\lambda f}$ obtained from eq. (43) when identifying $\omega^2_{\lambda c}$ with $\Gamma_{\lambda c}$. The value of $\gamma_{\lambda f}$ obtained from eq (37) and $\Gamma_{\lambda c} = \gamma^2_{\lambda c}$ are shown in column 5. Finally, column 6 contains the photon widths calculated in ref. [27]) from a table provided by Lynn [5]). The complex potential of ref. [26]) was used in evaluating (37) and (43).

$^{60}Ni(n,\gamma)$

E_λ (keV)	$\Gamma_{\lambda c}$ (keV)	$\Gamma_{\lambda f}$ (eV)	$\omega^2_{\lambda f}$ (eV)	$\gamma^2_{\lambda f}$ (eV)	Ref.[27]) (eV)
12	1.41	0.367	0.670	0.500	0.390
43	0.14	0.018	0.022	0.011	0.006
98	1.07	0.102	0.101	0.044	0.045
108	1.75	0.209	0.160	0.070	0.030
162	5.30	0.166	0.380	0.140	0.051
186	5.70	0.062	0.330	0.130	0.227
190	3.50	0.557	0.190	0.080	0.114

6 b. Dependence upon mass number

In fig. 2, we show the numerator (N) and denominator (D) of expression (43), in arbitrary units, and their ratio N/D (full curve), for the potential of ref. [26]). The dash-and-dots represent the ratio N/D for Moldauer's potential [29]). We see that the channel capture contribution is largest near $A = 60$. As discussed elsewhere by A.M. Lane, additional effects must, however, probably be invoked for explaining the predominance of channel capture in that region.

6 c. Choice of potential well

We mentioned in sect. 5 a that in practice the elastic scattering data are analyzed with the help of eqs. (17) and (39), with $Q^{(\infty)}_{cc} = 0$. Thus, it is only for the corresponding choice of v_o that $\gamma^2_{\lambda c}$ can be identified with the "experimental" neutron width. For a

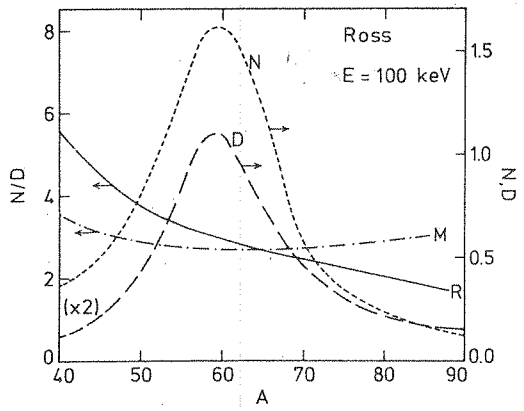

Fig. 2. Dependence upon mass number of the numerator (N) and denominator (D) of expression (43). The full curve refers to the ratio N/D for the potential of ref. [26]) and the dash-and-dots for the potential of ref. [29]).

fixed diffuseness, and a radius $R_o = r_o A^{1/3}$, it can be seen that the depth of this potential v_o must display a jump for some value of A, for low energy scattering. This is shown in fig. 3, where we plot versus A the depth of a real potential well [21]) which yields the same scattering length as the OMP of ref. [26]).

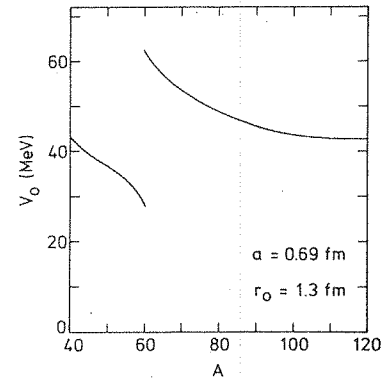

Fig. 3. Mass dependence of the depth of a real well which reproduces the experimental scattering length.

Hence, one must be careful in choosing the value of v_o. However, a large freedom exists provided that one uses a relation similar to eq. (41) to relate the experimental and theoretical width.

6 d. Background cross section

In refs. [25,28]), the direct cross-section corresponding to $S^{(o)}_{cf}$ (eq. (50)) was evaluated. This, however, differs from the background cross section $S^{(\infty)}_{cf}$, unless v_o is chosen in such a way that it fits the background (sect. 5 c). We have calculated from eq. (48) the

ickground cross section at 100 keV , for the potentials of refs. [26]) and [29]). The results are shown in fig. 4, in arbitrary units.

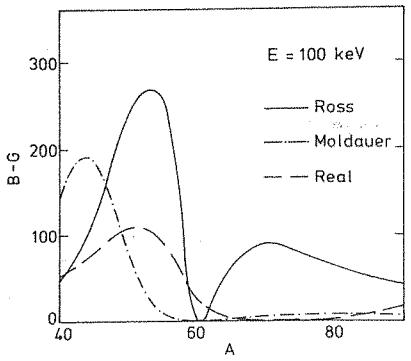

Fig. 4. Background cross section versus A , from the complex potentials of refs. [26,29]) (eq. (48)) and from the potential of fig. 3 (eq. (50)).

he long dashes show the value calculated from eq. (50), for the otential of fig. 3. We note that the background is quite sensitive o the choice of the potential. This reflects the importance of the urface region for this quantity [5,21]).

7. Conclusions

We have described some applications of the SMA to the theory of adiative capture. In the channel capture model, Lane and Mughabghab [2]) have shown that the main results can be obtained without using ny particular theoretical approach. Nevertheless, a dynamical approch is useful, for the following reasons. Firstly, the model for the verage S-matrix (sect. 5 b) must be justified (dominance of channel apture). Secondly, we mentioned that assumption (32) implies a spe-ific definition for the optical-model potential. Thirdly, it appears o us, but this is largely subjective, that the "physical" origin of he correlations is better understood in the frame of some dynamical pproach. In the present picture, it results from the admixture of hannel components into the resonance state Z_λ . Finally, we recall hat in light nuclei, the radiative capture of protons is often assued to proceed via direct capture. This has received astrophysical pplications [30]), and has recently been used for obtaining spectroscopic information on the final states [31]).

We gratefully acknowledge numerous discussions with E. Boridy nd stimulating criticism by A.M. Lane.

References

1) H. Feshbach, Ann. of Phys. 5 (1958) 357
2) H. Feshbach, Ann. of Phys. 19 (1962) 287
3) C. Mahaux and H.A. Weidenmüller, Shell-Model approach to nuclear reactions (North-Holland, Amsterdam, 1969)
4) R.F. Barrett, L.C. Biedenharn, M. Danos, P.P. Delsanto, W. Greiner and H.G. Wahsweiler, Rev. Mod. Phys. 45 (1973) 44
5) J.E. Lynn, The theory of neutron resonance reactions (Clarendon Press, Oxford, 1968)
6) B. Buck and A.D. Hill, Nucl. Phys. A95 (1967) 271
7) J. Raynal, M.A. Melkanoff and T. Sawada, Nucl. Phys. A101 (1967) 369
8) M. Marangoni and A.M. Saruis, Nucl. Phys. A132 (1969) 649
9) N. Van Giai and C. Marty, Nucl. Phys. A150 (1970) 593
10) J. Birkholz, Nucl. Phys. A189 (1972) 385
11) B. Goulard and J. Joseph, Canadian Journ. of Phys. 51 (1973) 2376
12) W.L. Wang and C.M. Shakin, Phys. Rev. C5 (1972) 1898
13) H. Feshbach and F. Iachello, Ann. of Phys. 84 (1974) 211
14) W.L. Wang and C.M. Shakin, Phys. Rev. Letters 30 (1973) 301
15) W.L. Wang and C.M. Shakin, Phys. Rev. C9 (1974) 2144
16) V. Gillet, M.A. Melkanoff and J. Raynal, Nucl. Phys. A97 (1967) 631
17) A. Goswami and R.D. Graves, Phys. Letters 39B (1972) 499
18) M. Marangoni, P.L. Ottaviani and A.M. Saruis, Phys. Letters 49B (1974) 253
19) E. Boridy and C. Mahaux, Nucl. Phys. A209 (1973) 604
20) E. Boridy and C. Mahaux, Nucl. Phys. A215 (1973) 605
21) J. Cugnon and C. Mahaux, to be published
22) A.M. Lane and S.F. Mughabghab, Phys. Rev. C10 (1974) 412
23) H. Feshbach, Statistical properties of nuclei, ed. J.B. Garg (Plenum Press, New York, 1972) p. 25
24) A.M. Lane, Ann. of Phys. 63 (1971) 171
25) E. Boridy and C. Mahaux, Phys. Letters 45B (1973) 81
26) A.A. Ross, H. Mark and R.D. Lawson, Phys. Rev. 102 (1956) 1613
27) M.R. Bhat, R.E. Chrien, S.F. Mughabghab and O.A. Wasson, Statistical properties of nuclei, ed. J.B. Garg, Contributed Papers (State University of New York at Albany, New York, 1971), p. 28.
28) C.M. Shakin and M.S. Weiss, Phys. Rev. 2C (1970) 1809
29) P.A. Moldauer, Phys. Rev. B135 (1964) 642
30) W.A. Fowler, G.R. Caughlan and B.A. Zimmermann, Ann. Rev. Astronomy and Astrophysics 5 (1967) 525
31) C. Rolfs, Nucl. Phys. A217 (1973) 29

DISCUSSION

me (chairman).

ank you very much Dr. Mahaux. I do not think I know anyone who can bring equations
ive so well especially after a heavy Dutch lunch, it is quite an achievement.
think any disagreements we may have are at the very technical level and quite
interesting to people, who would be looking for just positive things such as
at would one advise the experimenter who wanted to expose strong valence effects,
at target would one advise them to use and so on. I think it is true that to answer
ch questions we would agree very closely. The similarity of the curves shows that
e should look for strong background effects below the mass at which the background
oss section comes to zero.

haux.

actly.

ne.

ll, I should as a chairman not monopolize the discussion , so may I invite some
estions on this talk.

rg.

just wanted to know if you could tell me where you got the experimental numbers
r the ^{60}Ni that you showed in your slides.

haux.

took a table that Bhat, Chrien, Wasson and Mughabghab[27] published at the Albany
nference (Statistical Properties of Nuclei, ed. J.B. Garg (Plenum Press, New York,
72) and we took these numbers.

ghabghab.

s that is correct. The calculated numbers appeared in a contribution to the Albany
nference. These Contributions were printed in a report at the State University of
w York at Albany.

rg.

tried to do some keV neutron capture measurements in these nuclei at Lucas
ights and we found that some of these resonances which are observed in coincidence
th a transition to one final state may not be s-wave resonances since they are
t observed in total cross section measurements. I want to know whether in your
mparison of the data with your calculations you have taken the l-value of the
pturing state?

haux.

s, we assumed s-waves.

Jackson

We can fortunately take credit for the "crime". The ^{61}Ni radiation widths in your table are our threshold data (ANL). H.E. Jackson and E.N. Strait, private communication in ref. 27). I wish to make one other comment. We have focussed considerable effort with the threshold technique on measurements in the Cr and Ni region. We see large non-resonant cross sections for ^{53}Cr which is near the maximum values on your plot, and a very small non-resonance cross section for ^{61}Ni(γ,n), which lies near the minimum in your plot. I will speak of this Thursday morning.

Mahaux.

That is interesting. One interesting case that we did not investigate is lead. There is some background which has been fluctuating with time. I do no know to what extent it really exists and to what extent it can be understood. Yet it is certainly an interesting case as well.

Cvelbar.

I would like to ask Prof. Mahaux for the explanation of the strange behaviour of the real potential.

Mahaux.

I think that it is related to threshold effects, but we did not investigate this otherwise interesting problem yet.

Lane.

There is one supplemental comment, that I would like to make there. Is it so that this continuity just corresponds to a change of the principal quantum number?

Mahaux.

Yes.

Khanna.

In the very beginning after you had finished your talk, Prof. Lane asked you whether I thought we agreed as far as the valency model is concerned. I would like to make a query about that. When Prof. Lane talked this morning he was really very much interested in the fact that sp^{-1} or ps^{-1}, or whichever state, should really split off from the giant dipole state and should carry its own strength without contributing anything to the dipole itself. Now from what you showed actually it is not obvious at all that this was happening. As a matter of fact it appears to me that it is not happening in your particular situation. Is that right or not?

Mahaux.

I am not sure that I understand the question.

Khanna.

Well see, this morning when for example Prof. Lane was talking about the valency model, he was trying to get that the state which is the s-particle state or the p-particle is split-off, and he talked of essentially the mechanism that that particular particle-hole state will carry its own strength at low energies and

Lane (chairman).

Please slow down.

Khanna.

and it will not share its strength with the giant dipole state. Now what you

Mahaux.

Well in a way we do ignore the existence of the giant dipole resonance. So what we do is to presume that the strength is not transferred to the giant dipole resonance. In a way, that is an assumption that we introduced just because we do ignore it. I am not quite sure that I do completely understand the physical arguement of Dr. Lane, but in our framework, and that is probably what he says in different words, I would guess that the explanation of the fact that this part of the strength is not transferred to the giant dipole resonance is, that actually in all curves the external region of the nucleus by far gives the most important contribution, for instance to the photon width. Now the schematic model of Brown and Bolsterli really has to do with matrix elements which are computed in the internal region, so I do not know whether Dr. Lane would agree from the qualitative point of view as for this origin for the decoupling from the giant dipole resonance.

Lane.

Yes, I will.

Mahaux.

I would think that if the neutron would come inside the nucleus and then make the transition most of the time, then you would not have this decoupling. The fact is that the photon usually is emitted while the neutron is a little bit outside the nucleus, and there you have decoupling from the giant resonance.

Khanna.

That would seem to suggest that what you see essential as a valence model, you are essentially putting that as an assumption so you are not getting that as a consequence of your calculation.

Mahaux.

Yes, exactly.

Khanna.

So that would seem to suggest that if you had restricted for example at two situations there, only one-state wave functions are considered, this situation will not hold; you will not have a decoupling.

Mahaux.

Yes indeed, if I would compute the photon width from bound states, I would get very bad results.

Lane.

Let met finally put a question myself. In one picture you showed, that $\gamma_{\lambda f}/\gamma_{\lambda n}$ decreased with A across the mass region 40-70, agreeing with an effect found with the complex potential. Does your calculation suggest the reason for this decrease?

Mahaux.

Much more with the Ross-potential than with the Moldauer-potential. Whether this is sufficient to account for the symmetry you were talking about this morning, I do not know.

Lane.

I think that the fact that you are using the real potential there, would rather suggest that the origin of this staggering across the mass range may arise from just the change of ...

Mahaux.

Sorry, on that curve I used the Lane-Mughabghab formula with optical potential (laughter).

Lane.

You see this is the danger of this subject: positive feedback!